Three-body recombination in spin-polarized atomic hydrogen

L. P. H. de Goey, T. H. M. v. d. Berg, N. Mulders, H. T. C. Stoof, and B. J. Verhaar
Department of Physics, Eindhoven University of Technology, Eindhoven, The Netherlands

W. Glöckle
Institut für Theoretische Physik, Ruhr-Universität Bochum, Bochum, West Germany
(Received 4 March 1986)

In view of the failure of the Kagan dipole mechanism to explain the magnetic field dependence of the H+H+H recombination rate in spin-polarized atomic hydrogen, we consider an additional process, the so-called dipole-exchange mechanism. Two simple approaches to estimate its consequences turn out to be promising but the question of the role of different and higher-order processes remains open. We therefore turn to in principle, an exact approach to the three-body recombination, including all possible processes. The first numerical results of the approach are presented.

I. INTRODUCTION

In several laboratories experiments are being carried out with the ultimate aim of achieving Bose-Einstein condensation in spin-polarized atomic hydrogen (H↓). For these attempts to be successful, it is of vital importance to understand the decay mechanisms in H↓ samples. Former belief that the decay at low temperatures found in "precompression" experiments was due to two-body surface relaxation[1] led to large discrepancies between theory and experiment. Hess *et al.*[2] first came up with the interesting suggestion, that these discrepancies might be resolved, if three-body processes were taken into account. At high magnetic fields in the doubly polarized regime (both electron and proton spins polarized), where only b atoms (a,b,c,d are hyperfine levels of ground-state atomic hydrogen in order of increasing energy) are present, they found three-body rates of $L_g=7.5(3)\times10^{-39}$ $\mathrm{cm^6\,s^{-1}}$ in the volume, and $L_s=2.0(6)\times10^{-24}$ $\mathrm{cm^4 s^{-1}}$ at the surface at $B=7.6$ T, both decreasing slightly with magnetic field B.

Since it is now believed that this decay process represents the main obstacle on the way to achieve Bose-Einstein condensation, it seems worthwhile to find out by which mechanism(s) it takes place. In Sec. II the Kagan dipole mechanism,[3] the first mechanism proposed for a *bbb* three-body process is reviewed both for the volume[3] and for the surface.[4] The absolute magnitude of L_s is too small by an order of magnitude, and, more important, both L_g and L_s have a field dependence different from experiment. We therefore try to find an additional recombination mechanism both for the volume and the surface with a different B dependence, dominating the Kagan dipole mechanism for the volume and strongly dominating in the surface case. The most promising approach would be to first solve the volume discepancy. Once that recombination process is understood, it may be easier to deal with the surface. In Sec. III we therefore introduce a new mechanism, the socalled dipole-exchange mechanism, by which we hope to resolve the discrepancy. We find, however, that a naive approach to calculate its contribution leads to an overestimate by more than an order of magnitude. On the basis of this we then turn to an approach which treats the three-body aspects exactly. This is described in Sec. IV. In Sec. V the first numerical results of this approach are shown. A discussion follows in Sec. VI.

II. KAGAN DIPOLE MECHANISM

We consider the recombination of two H atoms in a three-body collision, taking place in a strong external magnetic field. As first discussed by Kagan *et al.*,[3] with all three atoms doubly polarized, this recombination is caused by an electron-electron magnetic dipole interaction. The idea is that the electron spins of two atoms precess in the magnetic dipole field of a third H atom, thus getting a total $S=0$ component, whereafter recombination is possible. The proton spins are unaffected during the process. The third atom is not only needed for this so-called spin flip, but also for conservation of the energy released during the recombination:

$$\frac{\mathbf{q}_f^2}{2(\frac{2}{3}m_{\mathrm{H}})}=-E_{vj}-2\mu_B B \quad (T\to 0)\,. \tag{1}$$

Here $-E_{vj}$ is the binding energy of the molecule in the final state with vibrational and rotational quantum numbers v and j, $2\mu_B B$ is the Zeeman energy needed for a single spin-flip process, μ_B is the Bohr magneton and $\mathbf{q}_f$ is the relative momentum of atom (mass m_{H}) and molecule. We shall restrict ourselves to $T\to 0$ calculations. In Eq. (1) and in the following we restrict ourselves for simplicity to the socalled single spin-flip process. With some obvious changes, such as the replacement of $2\mu_B B$ by $4\mu_B B$, similar expressions hold for double spin flip.

The most appealing feature of the calculation of Kagan *et al.* is its simplicity. The starting point is the exact "post form,"

$$f_{vjm}^{\sigma_f}(\mathbf{q}_f)=\frac{m_{\mathrm{H}}/9}{2\pi\hbar^2}\left\langle\phi_f\left|\sum_{k=2}^{3}V_k^d+\sum_{k=2}^{3}V_k^c\right|S\Psi_i^+\right\rangle\,, \tag{2}$$

for the scattering amplitude, vjm being the molecular quantum numbers (m is the magnetic quantum number), while σ_f is the final spin projection of the atom along **B**. Here V_k^d and V_k^c are the dipole and central interactions between the atoms of pair k (particles m and n with $m \neq k$ and $n \neq k$). The initial state Ψ_i^+, symmetrized using the symmetrization operator S (sum over six permutations without normalization coefficient), is in the first instance an exact scattering state of the total system, describing three atoms approaching one another with momenta which are considered to be small. The plane-wave part of Ψ_i^+ is normalized as an exponential with coefficient $(2\pi\hbar)^{-3}$. In Eq. (2), ϕ_f describes the free motion of atom 1 and the molecule consisting of atoms 2 and 3. Again its plane-wave factor is the usual exponential with coefficient $(2\pi\hbar)^{-3/2}$.

In terms of the amplitudes (2) the rate constant L_g for volume recombination has the form

$$L_g = \left\langle \sum_{v,j,m\sigma_f} \frac{9q_f}{m_{\mathrm{H}}} (2\pi\hbar)^9 \int d\hat{\mathbf{q}}_f \, | f_{vjm}^{\sigma_f}(\mathbf{q}_f) |^2 \right\rangle_{\text{thermal}} \tag{3}$$

where the integral is an angular integral over directions of $\mathbf{q}_f$. The corresponding expression for surface recombination has been given in Ref. 4.

Starting from Eq. (2) we now introduce the approximations of Kagan *et al.* The amplitude is calculated to first order in the weak dipole interaction, which is only taken into account in the form of the operator connecting initial and final state. A far-reaching simplification for Ψ_i^+ would consist of replacing it by its exponential free part. Instead Kagan *et al.* introduce some of the distortions, but in such a way that the final expression can still be handled fairly easily. Insofar as the initial state is operated upon by V_2^d, they consider the distortions of the relative motion of atom pair 2 as essential, as well as the distortion of the pair 1, since this pair is bound as a molecule in the final state. With this in mind they write the free exponential as a product of two exponentials in the corresponding relative coordinates and subsequently replace the exponentials by the corresponding distorted waves Ψ_t. The term with V_3^d is handled similarly. The contributions of the two terms cancel for j=even and are equal for j=odd.

Using these approximations the amplitude separates into two spatial matrix elements:

$$f_{vjm}^{\sigma_f}(\mathbf{q}_f) = C_j \langle \Psi_{vjm} \, | \, e^{i\mathbf{q}_f \cdot \mathbf{r}/2\hbar} \, | \, \Psi_t \rangle_1 \langle \mathbf{q}_f \, | \, V_\sigma^d \, | \, \Psi_t \rangle_2 \, , \tag{4}$$

where V_σ^d represents the spatial part of the dipole interaction: $Y_{2,-1}(\hat{\mathbf{r}})/r^3$ or $-2Y_{2,-2}(\hat{\mathbf{r}})/r^3$ for $\sigma = -\frac{1}{2}$ or $\sigma = +\frac{1}{2}$, respectively, while

$$C_j = -\frac{1}{(15\pi^3)^{1/2}} \frac{\mu_0 \mu_B^2 m_{\mathrm{H}}}{\hbar^2} \delta_{j,\text{odd}} \, . \tag{5}$$

The subscripts to the matrix elements in Eq. (4) indicate the particle pair to which each of the matrix elements applies. The second factor describes the action of the dipole interaction among particles 1 and 3 (1 and 2) giving rise to final momentum $\mathbf{q}_f$. The free relative state $|\mathbf{q}_f\rangle$ is again normalized as an exponential with coefficient $(2\pi\hbar)^{-3/2}$.

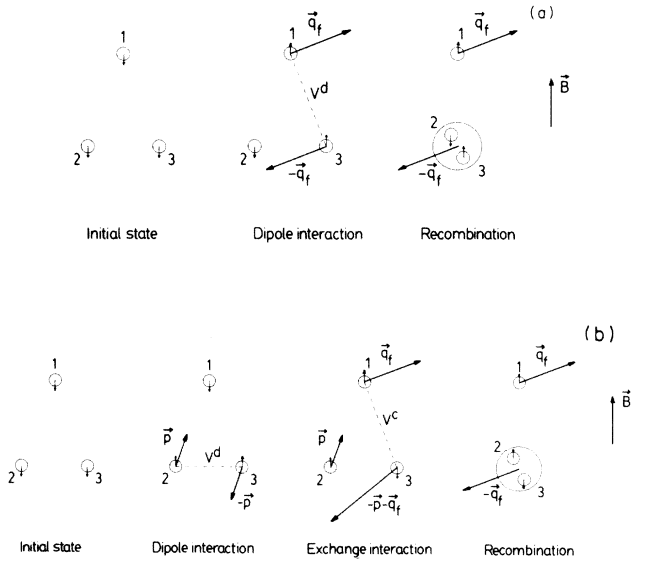

FIG. 1. (a) Graphical representation of the Kagan dipole process. The long arrows represent the momenta of the particles after the various stages of the process displayed. The short arrows represent spin angular momenta. (b) Graphical representation of the dipole-exchange process. Long arrows: momenta. Short arrows: spins.

The first factor describes the corresponding momentum change of particles 2 and 3 and the overlap with the final molecular state. A graphical representation of this so-called Kagan-mechanism is given in Fig. 1(a). Momenta are indicated by long arrows, spins by short arrows. In contrast to the equations in this paper, Figs. 1(a) and 1(b) illustrate double spin flip, which is somewhat easier to visualize.

The dipole interaction turns out to introduce only small momentum changes. Since q_f goes down with increasing B, the momentum mismatch decreases, leading the amplitude to increase in magnitude with B. The approach of Kagan *et al.* leads to a volume rate of $L_g = 8.5 \times 10^{-39}$ cm^{6}s^{-1} at $B = 10$ T and $T = 0$, increasing with B by a factor of 3 from 4–9 T.

The rate of this Kagan mechanism was also calculated for the surface case by de Goey *et al.*,[4] who found $L_s = 1.3 \times 10^{-25}$ cm^{6}s^{-1} at $B = 7.6$ T and $T = 0.4$ K, increasing by 70% from 4 to 9 T. The increase of these rates as a function of B, contrary to the experimental field dependence, has led us to investigate other mechanisms with non-negligible rate.

III. DIPOLE-EXCHANGE MECHANISM

An essential feature of the Kagan dipole mechanism is that the two particles, interacting via the dipole interaction cannot recombine, because this interaction only permits $S = 1$ to $S = 1$ transitions. The idea behind the dipole-exchange mechanism is that recombination between these particles is made possible, after that one parti-

cle has meanwhile changed its spin state by interaction with a third one via a strong exchange (triplet or singlet) interaction [see Fig. 1(b)].

We have estimated the rate for this process in two ways. The first one is a Kagan-like approach, the second one is an impulse-approximation-like calculation. We will discuss them in this order.

The idea of the first approach is to follow the approach of Kagan *et al.*[3] for exchange recombination, e.g., for *aab* scattering, but to consider dipole distorted states for the recombining atoms instead of hyperfine distorted states. We write the amplitude again as Eq. (2), but now we consider the remaining part of the operator consisting of the central interactions. The initial state Ψ_i^+ is now approximated to first order in the dipole interaction. Following Kagan *et al.* we replace Ψ_i^+ by a product of two triplet wave functions. The triplet function describing the initial motion of the recombining particles, is distorted with a dipole interaction. This changes Ψ_t into Ψ_t^d and produces the necessary spin flip(s), but no change of S. The subsequent spin exchange due to the V_2^c and V_3^c operators enables atoms 2 and 3 to recombine.

The amplitude for single spin flip ($\sigma_f=-\frac{1}{2}$) can now be written as [cf. Ref. 3 and Eq. (4)]

$$f_{vjm}^{\sigma_f=-1/2}(\mathbf{q}_f)=\tfrac{1}{2}C_j\langle\Psi_{vjm}\mid e^{i\mathbf{q}_f\cdot\mathbf{r}/2\hbar}\mid\Psi_t^d\rangle_1\langle\mathbf{q}_f\mid V^c\mid\Psi_t\rangle_2$$
$$=\tfrac{1}{2}C_j\int d\mathbf{p}\langle\Psi_{vjm}\mid\tfrac{1}{2}\mathbf{q}_f+\mathbf{p}\rangle_1\langle\mathbf{q}_f\mid V^c\mid\Psi_t\rangle_2\frac{1}{(p^2/m_{\mathrm{H}})+2\mu_B B}\langle\mathbf{p}\mid V_\sigma^d\mid\Psi_t\rangle_1 . \quad (6)$$

Here $\langle\mathbf{q}_f\mid V^c\mid\Psi_t\rangle_2$ and $\langle\mathbf{p}\mid V_\sigma^d\mid\Psi_t\rangle_1$ represent the action of central and dipole interactions, leading to final momenta $\mathbf{q}_f$ and $\mathbf{p}$, respectively. Furthermore, $\langle\Psi_{vjm}\mid\frac{1}{2}\mathbf{q}_f+\mathbf{p}\rangle_1$ is the overlap of the resulting state with momentum $\frac{1}{2}\mathbf{q}_f+\mathbf{p}$ of the recombining atom pair with the final molecular state. The energy denominator represents the free propagation in between the interactions. Figure 1(b) illustrates this approach, except for the $\mathbf{p}$ contribution to the momenta of the atoms 2 and 3, which for the time being is left out in the V^c matrix element. In a way, therefore, the present approach deals with the dipole and exchange interaction as parallel processes in sofar as the spatial degrees of freedom are concerned. For the spin degrees of freedom the order of the processes is as indicated in Fig. 1(b). Results for L_g are given in Fig. 2(a).

To introduce the second approach we first note that the V^c matrix element in Eq. (6) can be written as

$$\langle\mathbf{q}_f\mid V^c\mid\Psi_t\rangle_2=\langle\mathbf{q}_f\mid t^c\mid\mathbf{0}\rangle_2\quad(T\to 0) . \quad (7)$$

Writing it in such a way it indeed becomes clear that the momentum change of particle 3 in the dipole process is not taken into account in the subsequent exchange process. With this in mind we replace the t^c matrix element by $\langle\mathbf{q}_f+\frac{1}{2}\mathbf{p}\mid t^c\mid\frac{1}{2}\mathbf{p}\rangle_2$:

$$f_{vjm}^{\sigma_f=-1/2}(q_f)=\tfrac{1}{2}C_j\int d\mathbf{p}\langle\Psi_{vjm}\mid\tfrac{1}{2}\mathbf{q}_f+\mathbf{p}\rangle_1$$
$$\times\langle\mathbf{q}_f+\tfrac{1}{2}\mathbf{p}\mid t^c\mid\tfrac{1}{2}\mathbf{p}\rangle_2$$
$$\times\frac{1}{(p^2/m_{\mathrm{H}})+2\mu_B B}\langle\mathbf{p}\mid V_\sigma^d\mid\Psi_t\rangle_1 . \quad (8)$$

The replacement of $\mid\mathbf{0}\rangle$ by $\mid\frac{1}{2}\mathbf{p}\rangle$ introduces higher partial waves. For even (odd) partial waves contained in $\mid\frac{1}{2}\mathbf{p}\rangle$, t^c is effectively a triplet (singlet) t matrix. As we shall see in Sec. IV this expression (8), with $\mid\Psi_t\rangle$ replaced by the free state $\mid\mathbf{0}\rangle$ in the V^d matrix element, would be obtained as one of the first-order terms in the expansion for the exact transition amplitude in powers of t^c. However, we do not base our analysis on such an expression, since replacing $\mid\Psi_t\rangle$ by $\mid\mathbf{0}\rangle$ would lead to a strong unphysical increase of the amplitude: the triplet repulsion does no longer damp the small-distance $1/r^3$ dependence of V^d. Figure 1(b), now with the $\mathbf{p}$ contributions included, is a graphical representation of this second approach (8) for the dipole-exchange mechanism. The resulting L_g is presented in Fig. 2(b). The field range in this case has been restricted to 0—10 T. Note that the energy argument of the t^c matrix in Eq. (8) is the energy $-2\mu_B B-p^2/2m_{\mathrm{H}}$ of the free intermediate state for pair 2, whereas in the first approach it has value 0. It thus becomes clear that the exchange process in the first approach does not take advantage of the relative momentum $\frac{1}{2}\mathbf{p}$ acquired by the atoms 1 and 3 through the dipole interaction. As a consequence only the s-wave part of the relative pair 2 wave function participates in the exchange process. In addition the Zeeman energy for the spin flip(s) is produced by the dipole pair only, contrary to the second approach, where it is produced by all three particles.

These differences explain the much higher rate for the second approach. At a field of 8 T we find $L_g=2.8\times10^{-40}$ cm^{6}s^{-1} and $L_g=4.0\times10^{-38}$ cm^{6}s^{-1} for the first and second approach, respectively.

Turning from the absolute magnitude to the field dependence, we repeat that the dipole interaction can induce only small momentum changes. Therefore the integrals in Eqs. (6) and (8) are restricted to small p. Because of this we expect the rates to decrease with the field, mostly due to the denominator of the free propagator in Eqs. (6) and (8). This indeed appears to be the case. However, this field dependence is distorted in the first calculation by an additional zero of the exchange matrix element at $B=6$ T for the double spin-flip process and at $B=12$ T for the single spin-flip process [see Figs. 2(a) and 2(b)].

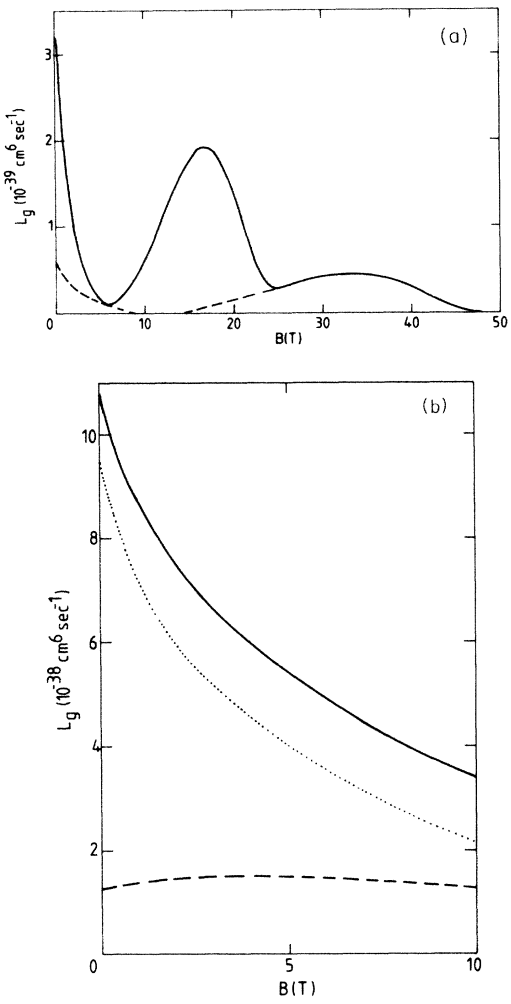

FIG. 2. (a) Three-body recombination rate L_g as a function of magnetic field B for the Kagan-like approach of the dipole-exchange process. The dashed curve represents the single spin-flip contribution, the full curve the sum of single and double spin-flip contributions. (b) Three-body recombination rate L_g as a function of B for the impulse-approximation-like approach of the dipole-exchange process. The dashed and dotted curves represent the contributions of the $v=14$, $j=3$ and $v=14$, $j=1$ final states to the total rate, respectively. The total rate is displayed by the full curve.

It may seem surprising that the rate of the second calculation is so large, roughly a factor of 5 larger than that of the Kagan dipole calculation. (This factor of 5 even increases to a factor of 20 if also other dipole-exchange terms are taken into account where the dipole interaction takes place between pair 2 if exchange occurs between pair 3 and vice versa.) Such large discrepancies seem to be common for calculations based on the impulse approximation.[5] This can be understood as follows. Considering the time-inversed process, i.e., the break-up process of a molecule colliding with an atom with relative momentum $-\mathbf{q}_f$, our impulse-like approximation means that the atom collides only with one atom of the molecule, while nothing happens with the other one, before the dipole interaction takes place. But this is very unlikely, especially for small q_f. The atom collides most probably with the molecule as a whole. In other words, rescattering processes, which are higher order in the t^c matrix, are important.

The shortcomings of the simple approaches (one underestimating the rate, caused by the approximations involved, the other giving rise to an overestimated rate, pointing to the fact that higher-order rescattering effects are important) force us to conclude that we are in need for a more exact three-body calculation, with all mechanisms and higher-order terms included. On the other hand, the field dependence found here gives us hope that the exact calculation will also give rise to a decreasing field dependence (higher-order rescatterings give rise to more free propagators with field B in the denominator). Such an approach is discussed in the remaining sections.

IV. EXACT THREE-BODY CALCULATION

In this section we describe a method for carrying out a three-body calculation of the *bbb* dipolar recombination process based on the Faddeev formalism,[6] in which the three-body aspects are dealt with exactly. In this calculation we take into account the strong central (singlet and triplet) interactions to all orders. The dipole interaction, however, only to first order. This is a very good approximation, because of the weakness of this interaction.[7]

Doing this, we can write the transition amplitude as

$$f^{\sigma_f}_{vjm}(\mathbf{q}_f)=\frac{m_H/54}{2\pi\hbar^2}\left\langle S\Psi_f^- \left| \sum_{k=1}^{3} V_k^d \right| S\Psi_i^+ \right\rangle . \tag{9}$$

Here, $|\Psi_i^+\rangle$ and $|\Psi_f^-\rangle$ are the initial and final states of the process, with central interactions taken into account to all orders, normalized as in the previous sections. We define the Faddeev components $|\chi_j\rangle$ as

$$G_0(E)V_j^c(1+P)|\Psi\rangle, \quad j=1,2,3 ,$$

where

$$|\Psi\rangle=(1+P_{23})|\Psi_i^+\rangle$$

for the initial state and

$$|\Psi\rangle=(1+P_{23})|\Psi_f^-\rangle$$

for the final state, P_{jk} standing for a permutation of particles j and k and P for $P_{12}P_{23}+P_{13}P_{23}$ (see Ref. 8). Also, $G_0(E)=1/(E-H_0)$ is the free propagator, H_0 being the free Hamiltonian, and E the total energy, both including Zeeman energy. The states $|\chi_j\rangle$ obey the Faddeev equations. For identical particles these equations reduce to equations, identical for all components. For $|\chi\rangle=|\chi_j\rangle$ this equation reads

$$|\chi\rangle=|\phi\rangle+G_0(E)t_1^c(E)P|\chi\rangle , \tag{10}$$

$t_1^c(E)$ being the central interaction t operator for pair 1. The driving term $|\phi\rangle=(1+P_{23})|\Psi_{vjm}\mathbf{q}_f\sigma_f\rangle_1$ describes the free motion of the molecule (pair 1) and atom 1 in spin state σ_f with relative momentum $\mathbf{q}_f$, when Eq. (10) is the Faddeev equation of the final state. For

the Faddeev equation of the initial state $|\phi\rangle = (1+P_{23})\,|\,\mathbf{p}_0^+\mathbf{q}_0 bbb\,\rangle_1$, describing pair 1 to be in a central interaction scattering state with momentum $\mathbf{p}_0$ and atom 1 moving freely with momentum $\mathbf{q}_0$ relative to pair 1. As usual the + sign describes outgoing wave boundary conditions at infinity. For $T\to 0$, the momenta $\mathbf{p}_0$ and $\mathbf{q}_0$ go to zero. The symmetrized states $S\,|\,\Psi_i^+\rangle$ and $S\,|\,\Psi_f^-\rangle$ in Eq. (9) can finally be found from the corresponding Faddeev components by operating with $1+P$.

To solve the above-mentioned two versions of Eq. (10) it is useful to introduce the angular-momentum basis[8] $|\,pq\alpha\rangle_j = |\,pq(l\lambda)LM_L(s\tfrac{1}{2})SM_S\,\rangle_j$, where p represents the magnitude of the relative momentum $\mathbf{p}$ of pair j, l their relative angular momentum quantum number, s their total spin quantum number, q the absolute magnitude of the relative momentum $\mathbf{q}$ of particle j with respect to pair j and λ the associated angular momentum quantum number, while LM_LSM_S stand for orbital and spin quantum numbers of the total system. Unless stated otherwise, this basis will be used with j equal to 1. For simplicity we therefore in general suppress the subscript 1.

In this basis the t operator for pair 1 in the three-particle space becomes

$$\langle\,pq\alpha\,|\,t_1^c(E)\,|\,p'q'\alpha'\,\rangle = t_{ls}^c\left[p,p',E-\frac{3q^2}{4m_{\mathrm{H}}}-2\mu_B BM_S\right]\frac{\delta(q-q')}{q^2}\delta_{\alpha\alpha'}\,, \tag{11}$$

where $t_{ls}^c(p,p',z)$ is the t matrix in the two-particle space:

$$\langle\,plm_lsm_s\,|\,t^c(z)\,|\,p'l'm_l's'm_s'\,\rangle = \delta_{ll'}\delta_{m_lm_l'}\delta_{ss'}\delta_{m_sm_s'}t_{ls}^c(p,p',z)\,. \tag{12}$$

The basis $\{\,|\,plm_lsm_s\,\rangle\}$ with m_l and m_s denoting orbital and spin magnetic quantum numbers, is normalized according to

$$\langle\,plm_lsm_s\,|\,p'l'm_l's'm_s'\,\rangle = \frac{\delta(p-p')}{p^2}\delta_{ll'}\delta_{m_lm_l'}\delta_{ss'}\delta_{m_sm_s'}\,. \tag{13}$$

The functions t_{ls}^c can be calculated with the Lippmann-Schwinger equation

$$t_{ls}^c(p,p',z) = V_{ls}^c(p,p') + \int_0^\infty dp''\frac{(p'')^2}{z-(p'')^2/m_{\mathrm{H}}} \times V_{ls}^c(p,p'')t_{ls}^c(p'',p',z)\,, \tag{14}$$

V_{ls}^c being the "Fourier transform" of the singlet or triplet interactions normalized according to an equation analogous to Eq. (12). For energies $z\le 0$, which are the only values appearing in the Faddeev equations for our initial and final states ($T\to 0$), the integral in Eq. (14) is regular and causes no problems. This one-dimensional integral equation can be solved by matrix inversion. When the energy $z=E-(3q^2/4m_{\mathrm{H}})-2\mu_B BM_S$ equals the energy E_{vj} of a two-particle bound state $v,j=l$, the t matrix has a pole in the singlet case ($s=0$). We come back to this problem shortly.

In the angular-momentum basis the particle permutation operator P in Eq. (10) has the representation[8]

$$\langle\,pq\alpha\,|\,P\,|\,p'q'\alpha'\,\rangle = {}_1\langle\,pq\alpha\,|\,p'q'\alpha'\,\rangle_2 + {}_1\langle\,pq\alpha\,|\,p'q'\alpha'\,\rangle_3 = \int_{-1}^{1}dx\frac{\delta(\pi_1-p)}{p^{l+2}}\frac{\delta(\pi_2-p')}{(p')^{l'+2}}G_{\alpha\alpha'}(q,q',x)\,, \tag{15}$$

with $\pi_1=[(q')^2+(q^2/4)+qq'x]^{1/2}$, $\pi_2=\{q^2+[(q')^2/4]+qq'x\}^{1/2}$, and

$$G_{\alpha\alpha'}(q,q',x) = \sum_{k=0}^{\infty}P_k(x)\sum_{l_1+l_2=l}\sum_{l_1'+l_2'=l'}q^{l_2+l_2'}q'^{l_1+l_1'}g_{\alpha\alpha'}^{kl_1l_1'l_2l_2'}\,. \tag{16}$$

The functions $P_k(x)$ are Legendre polynomials of the cosine x of the angle between $\mathbf{q}$ and $\mathbf{q}'$ and $g_{\alpha\alpha'}^{kl_1l_1'l_2l_2'}$ is the so-called geometrical factor, a complicated expression in terms of 3-j and 6-j symbols, for which we refer to Glöckle's monograph[8].

The remaining operator $G_0(E)$ in Eq. (10) has a simple form in the basis $|\,pq\alpha\,\rangle$:

$$\langle\,pq\alpha\,|\,G_0(E)\,|\,p'q'a'\,\rangle = \left[E-\frac{p^2}{m_{\mathrm{H}}}-\frac{3q^2}{4m_{\mathrm{H}}}-2\mu_B BM_S\right]^{-1}\frac{\delta(p-p')}{p^2}\frac{\delta(q-q')}{q^2}\delta_{\alpha\alpha'}\,. \tag{17}$$

For low temperatures, the energy $E=(p_0^2/m_{\mathrm{H}})+(3q_0^2/4m_{\mathrm{H}})-3\mu_B B<0$ approaches the energy for three polarized electron spins. Therefore for the final state, where $M_S=\pm\frac{1}{2}$, the energy factor in large parentheses in Eq. (17) is nonvanishing. For the initial state, on the other hand, the denominator vanishes when $p^2+3q^2/4 = p_0^2+3q_0^2/4$. This leads to singularities[9] in the kernel of the Faddeev equation (10). For $T\to 0$, however, the contribution of the singularities goes to zero continuously. We will come back to this problem shortly.

Equation (10) is a two-dimensional integral equation. The dimension of the kernel $G_0t_1^cP$ is too large to solve the equation by matrix inversion. Instead, we solve it by iteration (if the Neumann-series diverges, it is summed using Padé's method[10]). The successive terms in the series build in scattering correlations between the particles. Note that the final state $|\,\phi_f\,\rangle$ in our previous discussion of the Kagan dipole mechanism [see Eq. (2)] is just the driving term $|\,\phi\,\rangle$ of the Faddeev equation for the final state. The first iterated term $G_0t_1^cP\,|\,\phi\,\rangle$ is the state on

the left-hand side of the dipole interaction in the treatment of the dipole-exchange mechanism (Sec. III).

The advantage of the Faddeev equation is that its kernel is compact so that it has a unique solution.[11] The driving term $|\phi\rangle$, however, in general contains δ functions, which one cannot discretize. Therefore, instead of working with $|\chi\rangle$ we use another state $|\tilde{\chi}\rangle$. For the final state we write $|\tilde{\chi}\rangle = |\chi\rangle - |\phi\rangle$, which obeys

$$|\tilde{\chi}\rangle = G_0 t_1^c P |\phi\rangle + G_0 t_1^c P |\tilde{\chi}\rangle \ . \tag{18}$$

The driving term in this equation no longer contains δ functions. The driving term of the Faddeev equation of the initial state may be written as

$$\begin{aligned} |\phi\rangle &= (1+G_0 t_1^c)(1+P_{23})\,|\phi_0\rangle \\ &= (1+G_0 t_1^c)(1+P_{23})\,|\mathbf{p}_0\mathbf{q}_0 bbb\rangle \ , \end{aligned} \tag{19}$$

where $|\phi_0\rangle$ describes the free motion of three polarized atoms. We now define $|\tilde{\chi}\rangle$ as $|\chi\rangle - (1+P_{23})\,|\phi_0\rangle - G_0 t_1^c S\,|\phi_0\rangle$ and find $|\tilde{\chi}\rangle$ to obey the Faddeev equation

$$|\tilde{\chi}\rangle = G_0 t_1^c P G_0 t_1^c S\,|\phi_0\rangle + G_0 t_1^c P\,|\tilde{\chi}\rangle \ . \tag{20}$$

Once again δ functions have been eliminated from the driving term.

In Eqs. (18)–(20), G_0 and t_1^c have energy arguments E. Because of the poles of the t matrix (11) for $l=j$ at $(3q^2/4m_{\mathrm{H}}) = E - E_{vl} - 2\mu_B B M_S$, the kernel of the Faddeev equation (18) for the final state is irregular. These poles also occur in the solution $|\tilde{\chi}\rangle$. The physical meaning of these poles in the solution is that they are associated with waves extending to infinity in all open (elastic and inelastic) channels corresponding to the possible molecular states vj. The poles are handled in the following way. We define a new state $|\hat{\chi}\rangle$ by splitting off the pole factor from $|\tilde{\chi}\rangle$:

$$\langle pq\alpha\,|\,\hat{\chi}\rangle = \langle pq\alpha\,|\,\tilde{\chi}\rangle \times \prod_v \left[E - \frac{3q^2}{4m_{\mathrm{H}}} - E_{vl} - 2\mu_B B M_S - i\epsilon \right], \tag{21}$$

in which the product runs over all bound states with energy $E_{vl} < E - 2\mu_B B M_S$ for a certain angular momentum l. The poles in the driving term of Eq. (18) are eliminated in this way, but those in the kernel in the new integral equation for $|\hat{\chi}\rangle$ are not. The latter, however, can be handled by writing its kernel as a sum over individual pole terms and subsequently dealing with a pole at a specific q value q' by means of the following equation:

$$\int_0^\infty dq \frac{f(q)}{q^2-(q')^2-i\epsilon} = \int_0^\infty dq \frac{f(q)-f(q')}{q^2-(q')^2} + f(q') \int_0^\infty dq \frac{1}{q^2-(q')^2-i\epsilon} \tag{22}$$

for some regular function $f(q)$. Here the integrand of the first integral in the *rhs* is regular and the second term is easily calculated to be $-f(q')\pi i/2q'$.

The propagator G_0 in the initial state equation (20) gives rise to a singular behavior. Therefore we introduce a state $|\hat{\chi}\rangle = (E-H_0)\,|\tilde{\chi}\rangle$ for which we finally have the following Faddeev equation

$$|\hat{\chi}\rangle = t_1^c P G_0 t_1^c S\,|\phi_0\rangle + t_1^c P G_0\,|\hat{\chi}\rangle \ . \tag{23}$$

For $T \to 0$, the well-known singularity lines[9] in the kernel of this equation disappear.

V. FIRST NUMERICAL RESULTS

In this section we present the first results of an approach based on the method described in the preceding section. These calculations have been carried out by means of the local Eindhoven computer, with some exceptions for which we turned to the Cyber vector-array com-

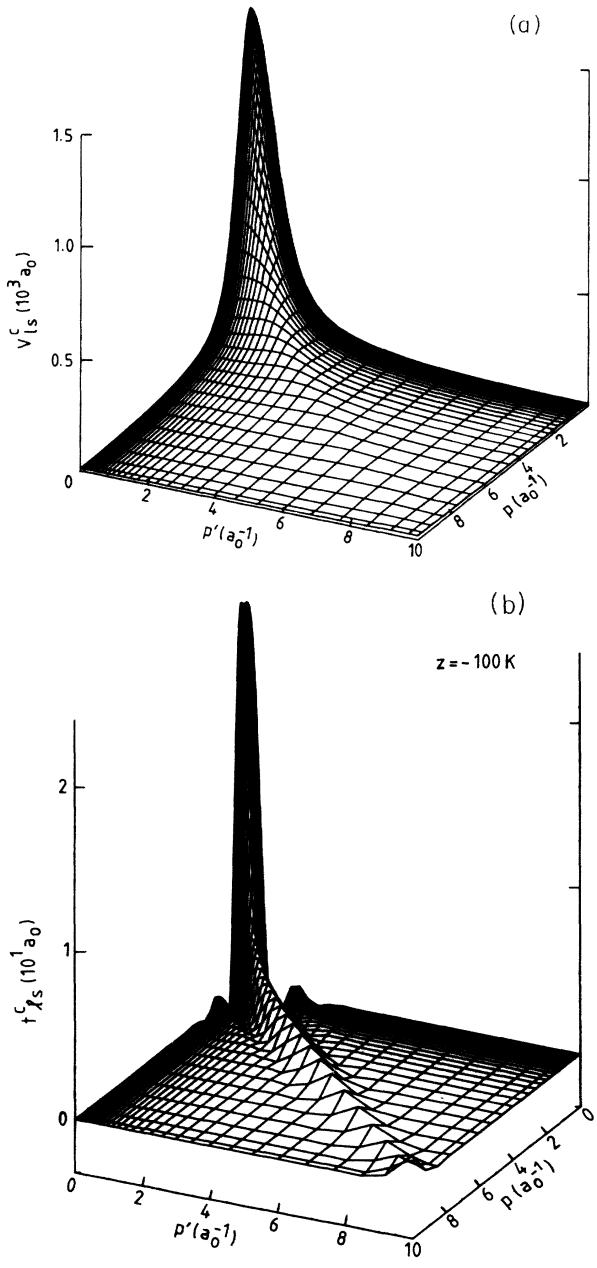

FIG. 3. (a) "Fourier transform" of the $l=0$ triplet potential $V_{ls}^c(p,p')$ as a function of final and initial momenta p and p'; (b) $l=0$ triplet t matrix $t_{ls}^c(p,p',z)$ as a function of p and p' for energy $z=-100$ K.

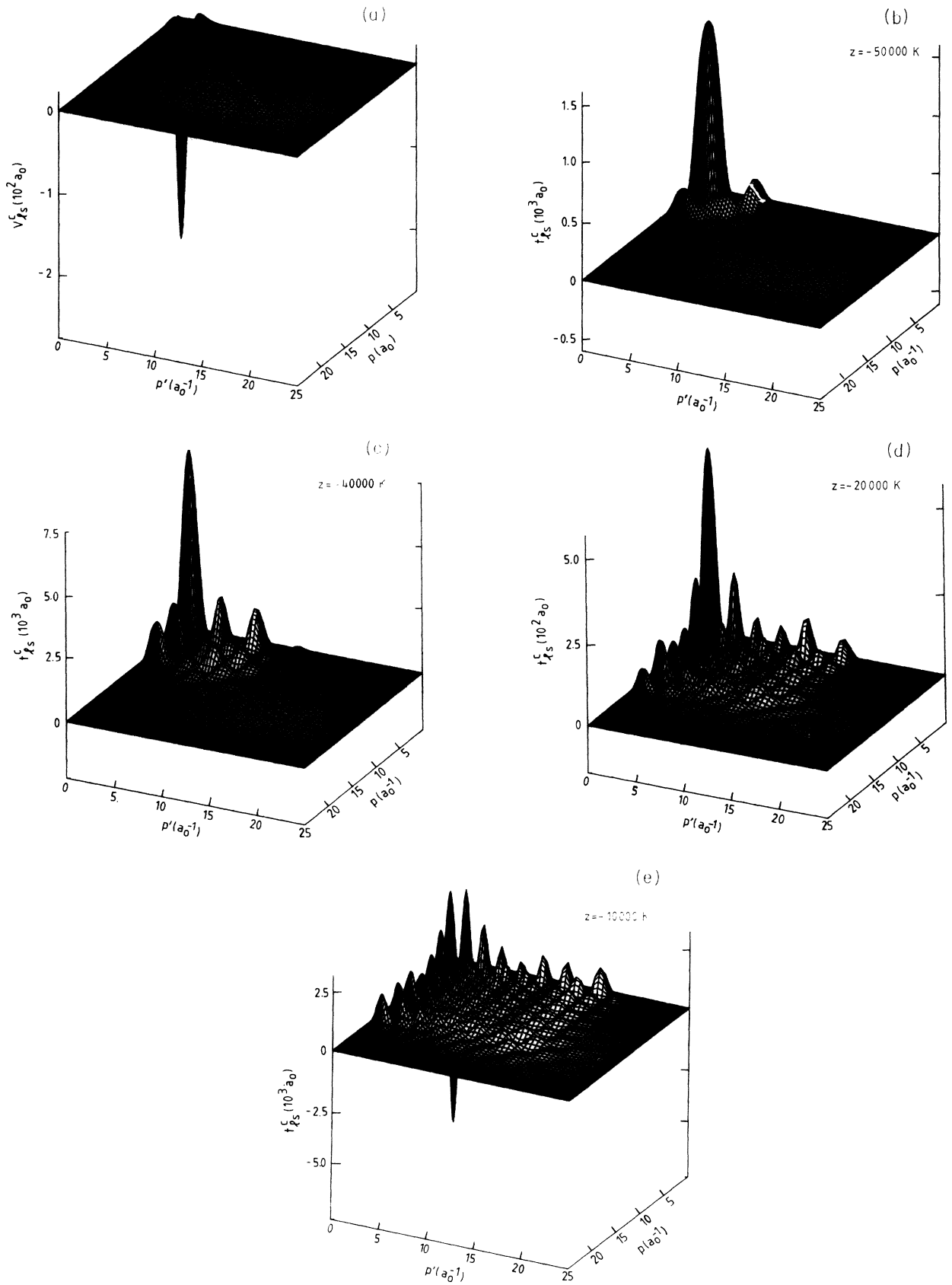

FIG. 4. (a) "Fourier transform" of the $l=1$ singlet potential $V_{ls}^{c}(p,p')$ as a function of p and p'; (b) $l=1$ singlet t matrix $t_{ls}^{c}(p,p',z)$ for energy $z=-50\,000$ K; (c) $l=1$ singlet t matrix $t_{ls}^{c}(p,p',z)$ for $z=-40\,000$ K; (d) $l=1$ singlet t matrix $t_{ls}^{c}(p,p',z)$ for $z=-20\,000$ K; (e) $l=1$ singlet t matrix $t_{ls}^{c}(p,p',z)$ for $z=-10\,000$ K.

puter of SARA in Amsterdam. The first step is the calculation of the functions $V^c_{ls}(p,p')$, the "Fourier transform" of the triplet and singlet potentials. These are shown in Fig. 3(a) for $s=1$, $l=0$ and in Fig. 4(a) for $s=0$, $l=1$. The second step is to calculate the t matrix with Eq. (14) by matrix inversion. As grid points we used Gauss-Legendre points. For the triplet case 75 grid points were sufficient. For the singlet case we used 121 points. A maximum momentum value of 35 a_0^{-1} turned out to be necessary. For the triplet potential, a value of 10 a_0^{-1} appeared to be sufficient. Special care has to be devoted to the choice of the "central" Gauss-Legendre point in the singlet case, due to the more complicated structure. As can be seen in Figs. 3(b) and 4(b)—4(e), where we present t^c_{ls} matrices for $s=1$, $l=0$ and $s=0$, $l=1$, respectively, we need more points for the singlet case, again because of the oscillations as a function of p and p'. For very low energies the oscillations disappear and less points are sufficient. However, energies near $z=0$ are likely to be more important for the solution of the Faddeev equations. We also calculated the residues $\hat{t}^c_{ls}(p,p',E_{vl})$ of the $t^c_{ls}(p,p',z)$ functions at the pole energies with the help of an additional equation:

$$\hat{t}^c_{ls=0}(p,p',E_{vl})=\langle plm_l \mid V^c \mid \Psi_{vlm_l}\rangle\langle \Psi_{vlm_l} \mid V^c \mid p'lm_l\rangle \ , \tag{24}$$

$|plm_l\rangle$ being the orbital part of the states $|plm_lsm_s\rangle$ with normalization corresponding to Eq. (13). The results of this calculation were in accordance with results from matrix inversion.

As a check on our program for solving the Faddeev equations we calculated the phase shift of elastic neutron-deuteron scattering at an energy $E_{\rm lab}=3.26$ MeV for a single α channel ($l=0$, $\lambda=0$, $L=0$, $s=1$, $S=\frac{3}{2}$, $M_S=\frac{3}{2}$, and isospin quantum numbers for pair 1 $t=0$ and total system $T=\frac{1}{2}$). We took this nuclear physics example, since similar calculations for atomic hydrogen are not available in the literature. The results were in accordance with results presented previously.[9]

To start with we did a one-channel calculation for the initial-state Faddeev equation (23), for which we needed 40×40 (p,q) grid points and found convergence after 20 iterations with Padé's method. We chose the most important $l=\lambda=L=0$, $S=\frac{3}{2}$, $M_S=-\frac{3}{2}$ channel. Because of the $1/q^2$ behavior of the driving term of Eq. (23), the solution $\hat{\chi}_\alpha(p,q)=\langle pq\alpha \mid \hat{\chi}\rangle$ also displays a $1/q^2$ dependence. This $1/q^2$ factor is cancelled by the q^2 phase-space factor of the matrix element in Eq. (9). For this reason and to see the underlying structure we plotted $q^2\hat{\chi}_\alpha(p,q)$ as a function of p and q in Fig. 5. This function is purely real, because of the disappearance of the singularities for $T\to0$, and obeys the "one channel" Schrödinger equation. We indeed checked that it fulfills that equation.

Furthermore, we did a preliminary one-channel calculation of the final state with 40×50 (p,q) points, in which we included eight poles of the kind mentioned in Eq. (21). We found convergence with Padé's method after 25 iterations. Clearly, the first results given in this section show

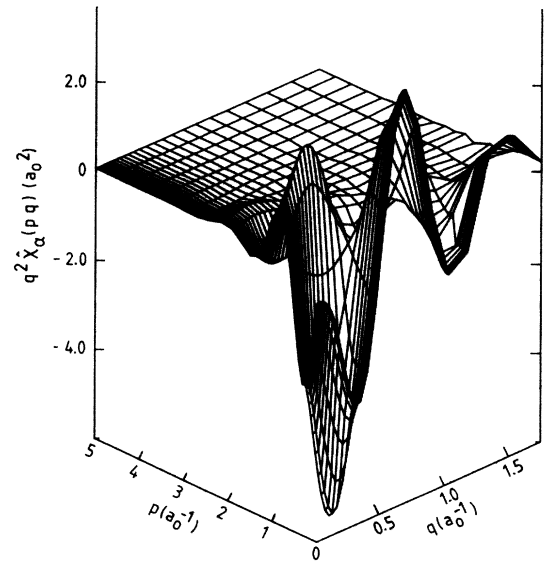

FIG. 5. Solution of the Faddeev equation (23) for the initial state, multiplied by q^2, i.e., $q^2\tilde{\chi}_\alpha(p,q)$ as a function of p and q for channel $\alpha=\{l=\lambda=L=0,\ S=\frac{3}{2},\ M_S=-\frac{3}{2}\}$.

the basic correctness of our method and also its feasibility when applied to atomic hydrogen.

VI. DISCUSSION

Anticipating a more complete approach extending the previous one-channel calculation, we now present some general considerations regarding the number of α channels to be taken into account. For the Faddeev equation of the initial state for $T\to0$, we have $s=1$, $S=\frac{3}{2}$, $M_S=-\frac{3}{2}$, $L=0$, and $l=\lambda$; so if l values ranging from 0 to $l_{\max}$ are to be included, we need about $l_{\max}/2$ channels (see Table I), because only even l values are possible. This is because of the fact that pairs of ground-state hydrogen atoms should have even $l+s+i$ for identical-particle reasons, where i is the total nuclear spin. With three b atoms in the initial state, $i=1$ for each atom pair. In our recombination process proton spins are unaffected.

For the final state the Faddeev equation is not as easy to solve, because we need a far greater number of channels. In Table I we see the number of channels needed as a function of the maximum l value $l_{\max}$. We now have both singlet and triplet channels. From the denominator of the propagator, the energy argument of the t matrix and the fact that the geometrical factor is independent of M_S, it can be concluded that the transition amplitude for the $M_S=+\frac{1}{2}$ channel ($\sigma_f=+\frac{1}{2}$) can be obtained from the $M_S=-\frac{1}{2}$ ($\sigma_f=-\frac{1}{2}$) channel by doubling the magnetic field B. We have an additional factor of -2 from the spin matrix element of the dipole interaction in Eq. (9):

$$f^{\sigma_f=+1/2}_{vjm}(B)=-2f^{\sigma_f=-1/2}_{vjm}(2B) \ . \tag{25}$$

As a consequence there is no need to calculate the field dependence for both M_S channels. In interpreting Table I it is of importance to point out that even and odd $l+\lambda$

TABLE I. Number of coupled channels as a function of the maximum angular momentum l_{max} for the initial- and final-state Faddeev equations.

State \ l_{max} =	0	1	2	3	4	5	· · ·	l_{max}
Initial	1	1	2	2	3	3	· · ·	$[l_{max}/2]+1$
Final	1	3	6	9	12	15	· · ·	$3l_{max}$

channels are uncoupled. This simplification of our three-particle problem follows from the diagonality of t^c and G_0 with respect to l and λ and from the fact that the geometrical factor does not couple even and odd $l+\lambda$. Furthermore, the initial state has even angular momentum quantum numbers $l=\lambda$ (otherwise not understandable) and the dipole interaction couples triplet channels only. As a consequence, only the $l+\lambda$ even channels are possible both for the initial and final states. From the conservation of total angular momentum $\mathbf{J}=\mathbf{L}+\mathbf{S}$, we would have both $L=1$ (i.e., $|l-1| \leq \lambda \leq l+1$) and $L=2$ (i.e., $|l-2| \leq \lambda \leq l+2$) channels. However, the dipole interaction transferring angular momentum $|\Delta\mathbf{L}| = |\Delta\mathbf{S}| = 2\hbar$ from spin to spatial degrees of freedom, only $L=2$ is allowed. These considerations lead to the dimensions of independent sets of coupled channels given in Table I.

From the considerations in Sec. III we may conclude that our so-called dipole-exchange mechanism is a potential candidate for solving the existing discrepancies of present theory and experimental recombination kinetics. In Sec. IV devoted to the principles of an exact approach, we have demonstrated that the building blocks of the Faddeev scheme, the potentials and t matrices with their complicated structure (see Fig. 4), can be controlled numerically. We have also shown that Faddeev equations can be solved under simplifying assumptions. The exploration of the rich content of physics contained in the process of recombination of three H atoms, including more and more channels, is under way using a vector-array computer. This should also answer the question whether three-body recombination is sufficiently suppressed at fields larger than about 25 T to allow Bose-Einstein condensation to be achieved in a compression experiment.

ACKNOWLEDGMENTS

The support of the Stichting Fundamental Onderzoek der Materie, The Netherlands (FOM) is gratefully acknowledged. This research was also supported by the stichting Nederlandse Organisatie voor Zuiver-Wettenschappelijk Onderzoek (The Netherlands) (ZWO) (Werkgroep Gebruik Supercomputers) and by the Government of the Land Nordrhein-Westfalen.

[1]R. M. C. Ahn, J. P. H. W. van den Eijnde, C. J. Reuver, B. J. Verhaar, and I. F. Silvera, Phys. Rev. B **26**, 452 (1982); J. P. H. W. van den Eijnde, C. J. Reuver, and B. J. Verhaar, *ibid.* **28**, 6309 (1983).

[2]H. F. Hess, D. A. Bell, G. P. Kochanski, D. Kleppner, and T. J. Greytak, Phys. Rev. Lett. **52**, 1520 (1984).

[3]Yu. Kagan, I. A. Vartan'yants, and G. V. Shlyapnikov, Zh. Eksp. Teor. Fiz. **81**, 1113 (1981) [Sov. Phys.—JETP **54**, 590 (1981)].

[4]L. P. H. de Goey, J. P. J. Driessen, B. J. Verhaar, and J. T. M. Walraven, Phys. Rev. Lett. **53**, 1919 (1984).

[5]M. I. Haftel and T. K. Lim (unpublished).

[6]L. D. Faddeev, Zh. Eksp. Teor. Fiz. **39**, 1459 (1961) [Sov. Phys.—JETP **12**, 1014 (1961)].

[7]R. M. C. Ahn, J. P. H. W. van den Eijnde, and B. J. Verhaar, Phys. Rev. B **27**, 5424 (1983).

[8]W. Glöckle, *The Quantum Mechanical Few-Body Problem* (Springer-Verlag, Berlin, Heidelberg, 1983), and references herein.

[9]W. M. Kloet and J. A. Tjon, Ann. Phys. (N.Y.) **79**, 407 (1973).

[10]G. A. Baker, *Essentials of Padé Approximants* (Academic, New York, 1975).

[11]F. Smithies, *Integral Equations* (Cambridge University Press, New York, 1958).

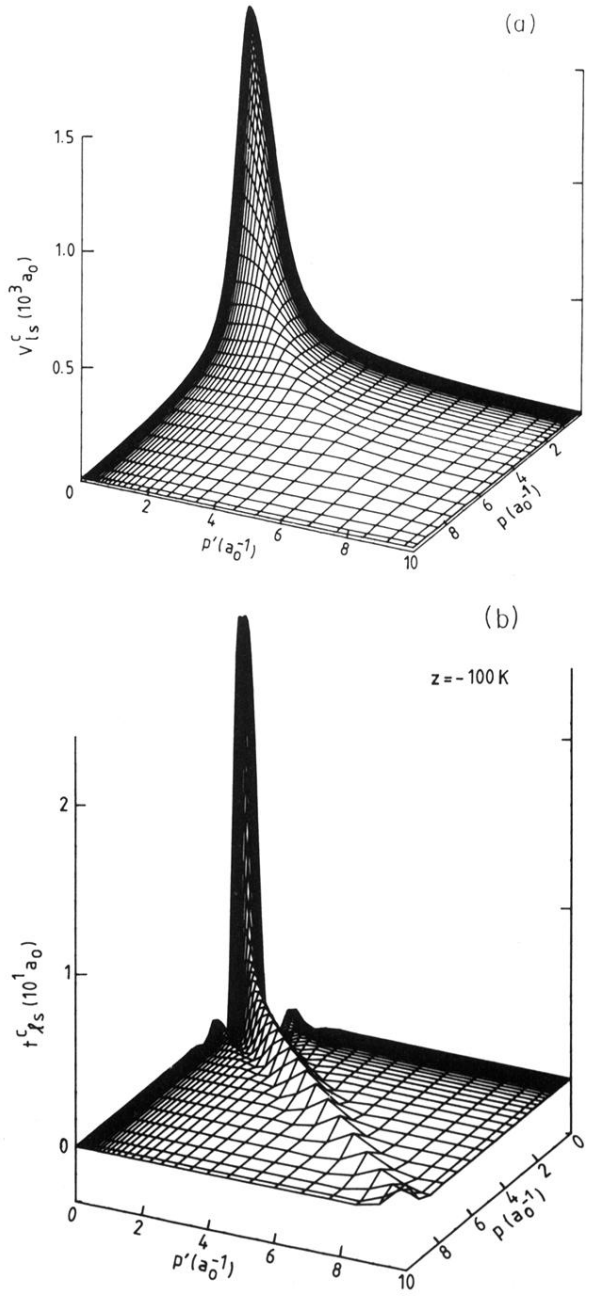

FIG. 3. (a) "Fourier transform" of the $l=0$ triplet potential $V^c_{ls}(p,p')$ as a function of final and initial momenta p and p'; (b) $l=0$ triplet t matrix $t^c_{ls}(p,p',z)$ as a function of p and p' for energy $z=-100$ K.

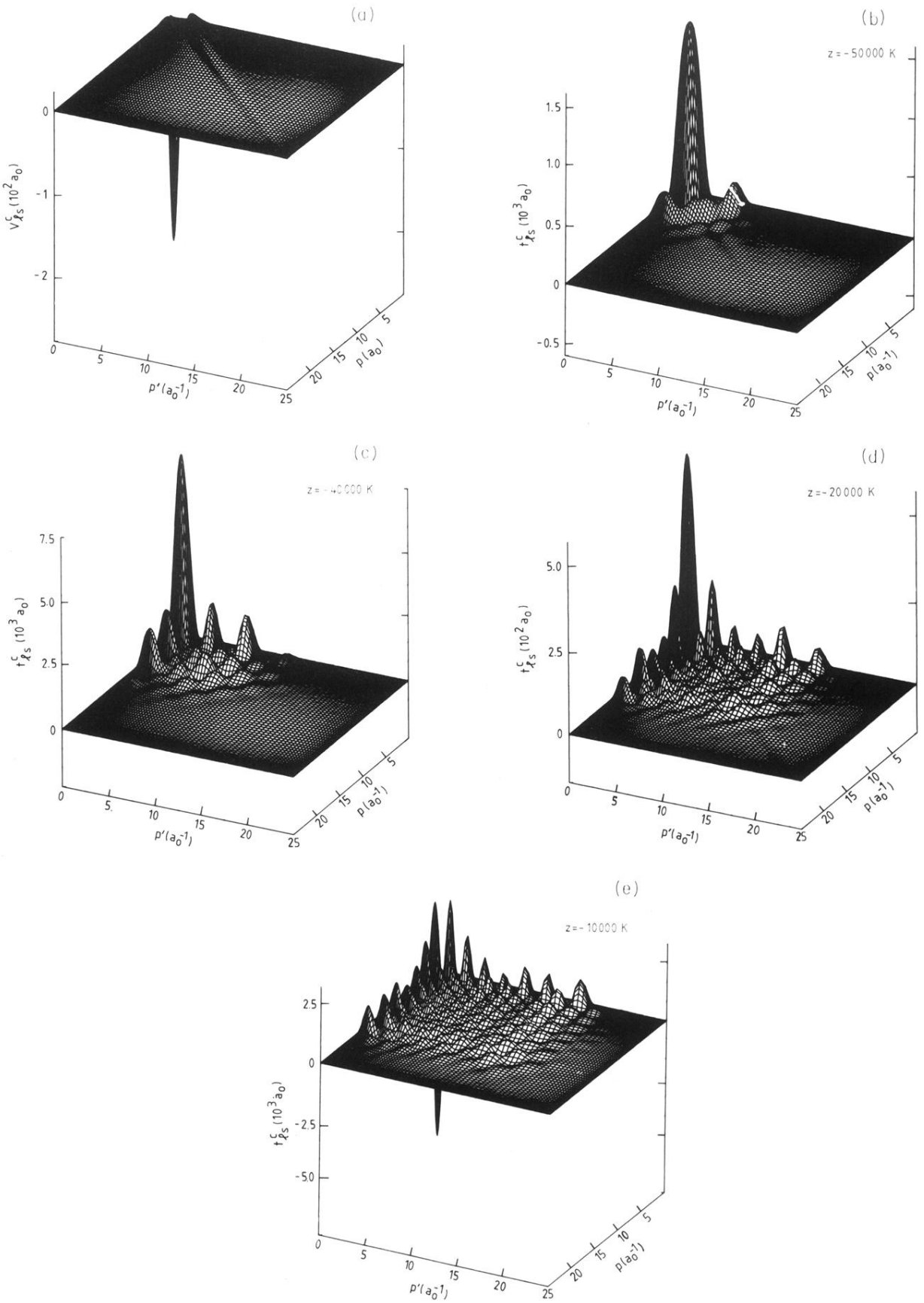

FIG. 4. (a) "Fourier transform" of the $l=1$ singlet potential $V_{ls}^{c}(p,p')$ as a function of p and p'; (b) $l=1$ singlet t matrix $t_{ls}^{c}(p,p',z)$ for energy $z=-50\,000$ K; (c) $l=1$ singlet t matrix $t_{ls}^{c}(p,p',z)$ for $z=-40\,000$ K; (d) $l=1$ singlet t matrix $t_{ls}^{c}(p,p',z)$ for $z=-20\,000$ K; (e) $l=1$ singlet t matrix $t_{ls}^{c}(p,p',z)$ for $z=-10\,000$ K.

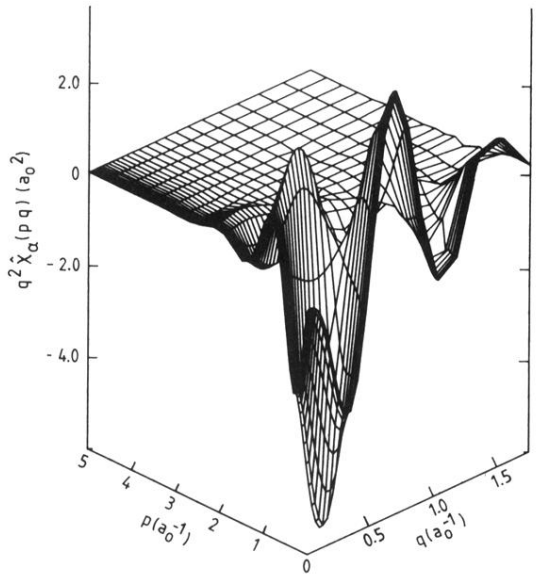

FIG. 5. Solution of the Faddeev equation (23) for the initial state, multiplied by q^2, i.e., $q^2\tilde{\chi}_\alpha(p,q)$ as a function of p and q for channel $\alpha=\{l=\lambda=L=0,\ S=\frac{3}{2},\ M_S=-\frac{3}{2}\}$.